in q, with a collision energy of 14 eV.

For second generation product ion spectra (sequential MS), appropriate settings of B and E were established to select first generation product ions (effective mass resolution 800) formed under metastable conditions in the first field-free region of the mass spectrometer[23] using a previously described instrument modification that permits independent control of E[4]. First generation product ions so selected were subjected to CAD in q (1.8×10^{-4} mbar of argon, 8 eV collision energy), with subsequent mass analysis of the second generation product ions with Q; 50–100 scans were accumulated by the data system in the MCA mode.

Mass deconvoluted MIKES analyses were obtained with the precursor ion selected by B, and with Q set to transmit the product ion of interest at unit mass resolution. E was then scanned over a narrow range, and 6–8 scans were accumulated. Metastable decomposition conditions were employed for these experiments.

Acknowledgment. The authors are grateful to Dr. Eddie Clayton (ICI Pharmaceuticals, Macclesfield, UK) and Prof. Michael L. Gross (University of Nebraska, Lincoln, NE) for useful discussions during these investigations. This work was supported in part through a generous gift from Glaxo, Inc.

Reactions of $(OC)_2Fe^{\bullet -}$ and $(OC)_3Mn^-$ with Cyclopropane: C–H Bond Activation, Dehydrogenation, and Deuterium Isotope Effects

Richard N. McDonald,* Michael T. Jones, and A. Kasem Chowdhury

Contribution from the Department of Chemistry, Kansas State University, Manhattan, Kansas 66506. *Received February 4, 1991*

Abstract: The reactions of cyclopropane with $(OC)_2Fe^{\bullet -}$ dihydrido-(c-C_3H_4) $(OC)_3Mn^-$ are unique among the hydrocarbons studied in that hydrido-(c-C_3H_5) and dihydrido-(c-C_3H_4) adduct products are observed accompaning those of dehydrogenation. The adduct and (adduct–H_2) product negative ion distributions are 35/65 from $(OC)_2Fe^{\bullet -}$ and 80/20 from $(OC)_3Mn^-$. The Fe-centered product ions were shown to be unsaturated and were characterized as $(OC)_2Fe(H)(c\text{-}C_3H_5)^{\bullet -}$ for the adduct, and $(OC)_2Fe(\pi\text{-}c\text{-}C_3H_4)^{\bullet -}$ or $(OC)_2Fe{=}\overline{CCH_2C}H_2^{\bullet -}$ for the (adduct–H_2) based on the results of their reactions with neutrals, e.g., D_2, Me_3SiH, and H_2S. The Mn-centered product ions did not react with these neutrals, suggesting that these ions are coordinatively saturated. The 18-electron dihydrido-(π-cyclopropene) structure likely represents the adducts, and $(OC)_3Mn(H)(\eta^3\text{-}c\text{-}C_3H_3)^-$ may represent the (adduct–H_2) ions. The extent of dehydrogenation was significantly reduced in the reactions with cyclopropane-d_6; general product structure (% from $(OC)_2Fe^{\bullet -}$, % from $(OC)_3Mn^-$): $(OC)_xM(D)(c\text{-}C_3D_5)^-$ (≈80, ≈20), $(OC)_xM(D)_2(c\text{-}C_3D_4)^-$ (≈9, ≈80), and $(OC)_xM(C_3D_4)^-$ (11, 0). The much smaller than expected kinetic isotope effect measured for the $(OC)_2Fe^{\bullet -}$ reactions (1.2 ± 0.1) is the result of the increased collisional quenching efficiency of the excited adducts $[(OC)_2Fe(D)(c\text{-}C_3D_5)^{\bullet -}]^*$ by the buffer gas. This secondary isotope effect reduces the return of the adducts to the starting ion and c-C_3D_6 that increases the rate of the cyclopropane-d_6 reaction masking the primary isotope effect for the insertion step. The larger isotope effect observed for the $(OC)_3Mn^-$ reactions (1.9 ± 0.3) is due to the normal isotope effect for the additional intramolecular deuterium shift step required to give the major adduct product ions. The reactivity of the cyclopropane C–H bonds suggest that the M–(c-C_3H_5) bond energy is greater than that for a secondary alkyl group in these negative ion complexes.

Intermolecular C–H bond activation with unsaturated transition-metal complexes is now a relatively common process with a number of examples in the literature.[1-10] However, success in intermolecular C–C bond activation is rare. It appears that both kinetic and thermodynamic factors are important for the cleavage of C–C bonds. A larger kinetic barrier is assumed for C–C bond activation than for the oxidative insertion into C–H bonds by transition-metal centers.[1b,11] Several indirect approaches using cyclopentadienes and even 1,1-dimethylcyclopentane[12] have led to products of C–C bond cleavage. In each case, the generation of the metal–alkyl bond occurs by rearrangement of a cyclopentadiene intermediate complex by an alkyl shift forming the corresponding Cp derivative; aromatization of the C_5 ring is the driving force.

Direct C–C bond activation has required strained alkanes, e.g., cyclopropane, where relief of the ring strain may facilitate the reaction,[1b,12] but depends on the strain in the product metallocycloalkane. Periana and Bergman[13] have shown that formation of $(\eta^5\text{-}C_5Me_5)(Me_3P)\text{-}\overline{Rh\text{-}CH_2CH_2C}H_2$ in the reaction of $(\eta^5\text{-}C_5Me_5)(Me_3P)Rh$ and cyclopropane proceeds by thermal rearrangement of the hydrido-cyclopropyl intermediate. The gas-phase reactions of Sc^+,[14] Y^+,[14] La^+,[14] Gd^+,[15] and $(\eta^5\text{-}c\text{-}C_5H_5)Co^+$[16] and cyclopropane occur predominately or exclusively by dehydrogenation.

C–H bond activation studies and dehydrogenation of alkanes containing C–H bonds β to the insertion site, cyclopentane, and

---

(1) For some recent reviews on this topic, see: (a) Ryabov, A. D. *Chem. Rev.* **1990**, *90*, 403. (b) Crabtree, R. H. *Chem. Rev.* **1985**, *85*, 245. (c) Halpern, J. *Inorg. Chim. Acta* **1985**, *57*, 1897. (d) Green, M. L. H.; O'Hare, D. *Pure Appl. Chem.* **1985**, *57*, 1897. (e) Rothwell, I. P. *Polyhedron* **1985**, *4*, 177. (f) Shilov, A. E. *The Activation of Saturated Hydrocarbons by Transition Metal Complexes*; Reidel: Dordrecht, 1984. (g) Parshall, G. W. *CHEMTECH* **1984**, *14*, 628. (h) Muetterties, E. L. *Chem. Soc. Rev.* **1983**, *12*, 283. (i) Brookhart, M.; Green, M. L. H. *J. Organomet. Chem.* **1983**, *250*, 395.

(2) (a) Janowicz, A. H.; Bergman, R. G. *J. Am. Chem. Soc.* **1982**, *104*, 352. (b) Janowicz, A. H.; Bergman, R. G. *J. Am. Chem. Soc.* **1983**, *105*, 3929.

(3) Hoyano, J. K.; Graham, W. A. G. *J. Am. Chem. Soc.* **1982**, *104*, 3723.

(4) (a) Jones, W. D.; Feher, F. J. *J. Am. Chem. Soc.* **1982**, *104*, 4240. (b) Jones, W. D.; Feher, F. J. *J. Am. Chem. Soc.* **1984**, *106*, 1650.

(5) Janowicz, A. H.; Periana, R. A.; Buchanan, J. M.; Kovac, C. A.; Stryker, J. M.; Wax, M. J.; Bergman, R. G. *Pure Appl. Chem.* **1984**, *56*, 13.

(6) Periana, R. A.; Bergman, R. G. *J. Am. Chem. Soc.* **1986**, *108*, 7332.

(7) Sponsler, M. B.; Weiller, B. H.; Stoutland, P. O.; Bergman, R. G. *J. Am. Chem. Soc.* **1989**, *111*, 6841.

(8) Fryzuk, M. D.; Jones, T.; Einstein, F. W. D. *Organometallics* **1984**, *3*, 185.

(9) Nubel, P. O.; Brown, T. L. *J. Am. Chem. Soc.* **1984**, *106*, 644.

(10) Jones, W. D.; Feher, F. J. *J. Am. Chem. Soc.* **1982**, *104*, 4240.

(11) Blomberg, M. R. A.; Siegbahn, P. E. M.; Nagashima, U.; Wennerberg, J. *J. Am. Chem. Soc.* **1991**, *113*, 424.

(12) Crabtree, R. H.; Dion, R. P.; Gibboni, D. J.; McGrath, D. V.; Holt, E. M. *J. Am. Chem. Soc.* **1986**, *108*, 7222 and references therein.

(13) (a) Periana, R. A.; Bergman, R. G. *J. Am. Chem. Soc.* **1984**, *106*, 7272. (b) Periana, R. A.; Bergman, R. G. *J. Am. Chem. Soc.* **1986**, *108*, 7346 references therein.

(14) Huang, Y.; Wise, M. B.; Jacobson, D. B.; Freiser, B. S. *Organometallics* **1987**, *6*, 346.

(15) Schilling, J. B.; Beauchamp, J. L. *J. Am. Chem. Soc.* **1988**, *110*, 15.

(16) Jacobson, D. B.; Freiser, B. S. *J. Am. Chem. Soc.* **1985**, *107*, 7399.

0002-7863/92/1514-71$03.00/0

Table I. Summary of Kinetic and Primary Product Data for the Reactions of $(OC)_3Mn^-$ and $(OC)_2Fe^{\bullet-}$ with Cyclopropane

rx. no.	neutral reactant	product ion [+assumed neutral(s)]	branching fraction	k_{total},[a] cm^3 $molecule^{-1}$ s^{-1}	k_{LAN},[b] cm^3 $molecul^{-1}$ s^{-1}	reaction efficiency[c]
$(OC)_3Mn^-$						
(1a)	$c\text{-}C_3H_6$	$(OC)_3Mn(H)_2(c\text{-}C_3H_4)^-$	0.80	$(4.1 \pm 0.3) \times 10^{-11}$	9.7×10^{-10}	0.042
(1b)		$(OC)_3Mn(c\text{-}C_3H_4)^-$ [+H_2]	0.20			
(2)	$c\text{-}C_3D_6$	$(OC)_3Mn(C_3D_6)^-$[e]	1.00	$(2.1 \pm 0.1) \times 10^{-11}$[d]		0.022
$(OC)_2Fe^{\bullet-}$						
(3a)	$c\text{-}C_3H_6$	$(OC)_2Fe(H)(c\text{-}C_3H_5)^{\bullet-}$	0.35	$(8.6 \pm 0.3) \times 10^{-11}$	1.0×10^{-9}	0.086
(3b)		$(OC)_2Fe(c\text{-}C_3H_4)^{\bullet-}$ [+H_2]	0.65			
(4a)	$c\text{-}C_3D_6$	$(OC)_2Fe(C_3D_6)^{\bullet-}$[e]	0.89	$(7.1 \pm 0.2) \times 10^{-11}$		0.071
(4b)		$(OC)_2Fe(c\text{-}C_3D_4)^{\bullet-}$ [+D_2]	0.11			

[a] These values are averages of at least two separate measurements. The listed errors are the maximum deviations in the measured rate constants from this average value, which is generally <±10%. The errors due to systematic uncertainties in calibrations suggest that their accuracy is ±20% for external comparisons. [b] The collision limited rate constants were calculated by the Langevin theory, k_{LAN}. See: Su, T.; Bowers, M. T. In *Gas Phase Ion Chemistry*; Bowers, M. T., Ed.; Academic Press: New York, 1979; Vol. 1, Chapter 3. [c] Defined as k_{total}/k_{LAN}. [d] k_{app} for the formally termolecular adduct forming reaction. [e] See text for a description of the structures of these adduct ions.

cyclohexane with $(OC)_3Mn^-$ and $(OC)_2Fe^{\bullet-}$ were recently reported.[17] These observations prompted us to examine the reactions of these two fragment metal carbonyl negative ions with cyclopropane to determine (a) if oxidative insertion into the strong $c\text{-}C_3H_5\text{–}H$ bonds would occur, and (b) if C–C bond activation would be a competitive reaction channel. The results of this study and the effects of deuterium substitution using cyclopropane-d_6 are reported herein.

Experimental Section

Our gas-phase studies are carried out in a previously described flowing afterglow (FA) apparatus at 298 K.[18] The conditions have been described to separately generate $(OC)_4Fe^{\bullet-}$ and $(OC)_5Mn^-$, and mixtures of $(OC)_{4,3}Fe^{\bullet-}$ or $(OC)_{4,3,2}Fe^{\bullet-}$, and $(OC)_{5,4}Mn^-$ or $(OC)_{5,4,3}Mn^-$ by dissociative attachment of electrons of different energies with $Fe(CO)_5$ and $Mn_2(CO)_{10}$, respectively, in a fast flow of helium buffer gas ($P_{He} \approx 0.9$ Torr, $\bar{v} \approx 57$ m s^{-1}).[17] Variations in P_{He} in these experiments are very limited in order to retain the ion signals of the ion mixtures containing $(OC)_2Fe^{\bullet-}$ and $(OC)_3Mn^-$. It is fortunate that the relatively high P_{He}, which is necessary to obtain the signals of the latter two ions, facilitates observation of adduct product ions formed in the reactions of the metal carbonyl anions with neutral substrates. The fragment metal carbonyl negative ions are cooled to their electronic and vibrational ground states by multiple collisions with the helium buffer gas in their flight down the first 75 cm of the flow tube.[19] Cyclopropane[20] is added via a radial inlet and the ion/molecule reactions occur in the final 65 cm of the flow tube. The flow is maintained by a large, fast-pumping system. The flow is sampled via 1-mm orifices in two nose cones into a differentially pumped chamber ($P \approx 10^{-7}$ Torr) containing a quadrupole mass filter and electron multiplier which continuously monitor the ion composition of the flow. The neutral products of these reactions are not directly observed, but are assumed based on thermochemistry and mass balance. Endothermic reactions are not observed in these gas-phase reactions, and the magnitudes of the rate constants are generally related to the reaction exothermicities.

The kinetics of these reactions are determined under pseudo-first-order conditions where the concentration of the cyclopropane added is always in large excess compared to the ion concentration. The slopes of the plots of log [starting ion signal] versus increasing cyclopropane concentration added to the flow yield the bimolecular rate constants by equations already given.[18b] The isotopic purity of the cyclopropane-d_6 was >98% (MSD).

Results

No reaction was observed between cyclopropane and the negative ion complexes $(OC)_{5,4}Mn^-$ and $(OC)_{4,3}Fe^{\bullet-}$. The kinetic and primary product data for the reactions of the 14-electron $(OC)_3Mn^-$ and 13-electron $(OC)_2Fe^{\bullet-}$ are given in Table I. In all of the experiments, linear pseudo-first-order decays of the starting ions were observed in the plots of log [ion signal] versus concentration of cyclopropane. This is illustrated in Figure 1 for the reaction of $(OC)_3Mn^-$ with cyclopropane. The integrals of the product ion signals accounted for >90% of the loss of the starting ion signal. The branching fractions given in Table I and in equations in the Discussion are the relative product ion signal intensities obtained by integration of the negative ion spectra (averages of 10 to 15 spectra to increase singal-to-noise ratios) taken for six to eight different concentrations of cyclopropane. The error in these branching fractions is ±3% absolute within the individual and the separate kinetic runs used to determine the average rate constants.

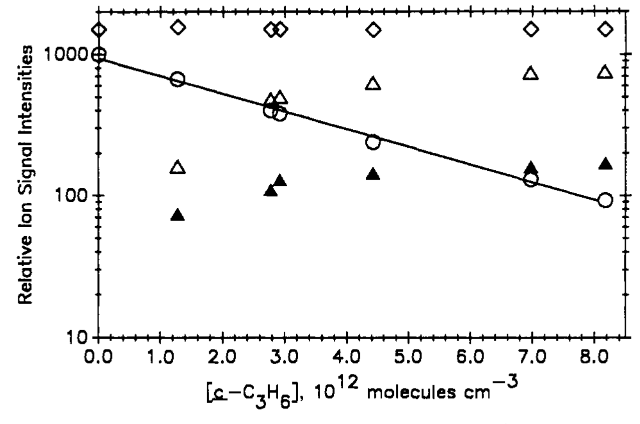

Figure 1. Semilog plot for the reaction of $(OC)_3Mn^-$ with cyclopropane; $(OC)_4Mn^-$ (◇), $(OC)_3Mn^-$ (○), $(OC)_3Mn(H)_2(c\text{-}C_3H_4)^-$ (△), and $(OC)_3Mn(c\text{-}C_3H_4)^-$ (▲).

Several of the product forming reaction channels involve adduct product ions. For these channels to be observed, removal of the excess energy in forming the adduct structure is required by collisions with the helium gas, or the adduct will dissociate. The apparent bimolecular rate constants, k_{app}, are reported for those reactions where this is the exclusive reaction channel because of our inability to significantly vary P_{He}.

Although the results were conclusive for the reactions used to structurally characterize the adduct and (adduct-H_2) ion products formed with cyclopropane, the presence of ≤5% of ions *unreactive* with the added neutral reagent could not be ruled out.

Discussion

Reactions with Cyclopropane. $(OC)_2Fe^{\bullet-}$ and $(OC)_3Mn^-$ reacted with cyclopropane with similar modest rate constants to yield mixtures of adduct and (adduct–H_2) ion products (eq 1 and 2).

$$\underset{m/z\ 112}{(OC)_2Fe^{\bullet-}} + c\text{-}C_3H_6 \xrightarrow[0.35]{He} \underset{m/z\ 154}{(OC)_2Fe(H)(c\text{-}C_3H_5)^{\bullet-}} \quad (1a)$$

$$\xrightarrow[0.65]{} \underset{m/z\ 152}{(OC)_2Fe(C_3H_4)^{\bullet-}} + H_2 \quad (1b)$$

---

(17) McDonald, R. N.; Jones, M. T.; Chowdhury, A. K. *J. Am. Chem. Soc.* **1991**, *113*, 476.

(18) (a) McDonald, R. N.; Chowdhury, A. K. *J. Am. Chem. Soc.* **1985**, *107*, 4123. (b) McDonald, R. N.; Chowdhury, A. K.; Setser, D. W. *Ibid.* **1980**, *102*, 6491.

(19) (a) McDonald, R. N.; Jones, M. T.; Chowdhury, A. K. *Organometallics*, in press. (b) McDonald, R. N.; Jones, M. T.; Chowdhury, A. K. *Organometallics*, in press.

(20) The cyclopropane (Matheson, 98.5 minimum purity) used in these experiments did not contain propene or other reactive impurities. Propene readily reacts with $(OC)_3Fe^{\bullet-}$ and more slowly with $(OC)_4Mn^-$ to form adducts[19b] that were not observed in the present experiments.

$$\underset{m/z\ 139}{(OC)_3Mn^-} + c\text{-}C_3H_6 \xrightarrow[0.80]{He} \underset{m/z\ 181}{(OC)_3Mn(H)_2(c\text{-}C_3H_4)^-} \quad (2a)$$

$$\xrightarrow[0.20]{} \underset{m/z\ 179}{(OC)_3Mn(c\text{-}C_3H_4)^-} + H_2 \quad (2b)$$

Both of the product ions formed in reaction 1 were observed to react rapidly with Me_3SiH[19a] and H_2S[17] when these neutrals were added via a port downstream of the cyclopropane addition port. The results of these reactions with the adduct at *m/z* 154 (eq 1a) are shown in eq 3 and 4. The structure of the (adduct–H_2) ions

$$\underset{m/z\ 154}{(OC)_2Fe(H)(c\text{-}C_3H_5)^{\bullet-}} + H_2S$$

$$\xrightarrow[0.83]{} \underset{m/z\ 186}{(OC)_2Fe(c\text{-}C_3H_5)(H)({=}S)^{\bullet-}} + H_2 \quad (3a)$$

$$\xrightarrow[0.17]{He} \underset{m/z\ 188}{(OC)_2Fe(H)_2(c\text{-}C_3H_5)(SH)^{\bullet-}} \quad (3b)$$

$$\underset{m/z\ 154}{(OC)_3Fe(H)(c\text{-}C_3H_5)^{\bullet-}} + Me_3SiH \rightarrow$$

$$\underset{m/z\ 226}{(OC)_2Fe(c\text{-}C_3H_5)(H)(\eta^2\text{-}CH_2{=}SiMe_2)^{\bullet-}} + H_2 \quad (4)$$

at *m/z* 186 (eq 3a) is our best guess. Since the *m/z* 186 ions did not react further with excess H_2S, we assume they are saturated. The β-hydrogen shift from a Me_3Si–ligand bound to an unsaturated metal center producing the hydrido-(π-(2-methyl-2-silapropene)) complex shown for the product ions of reaction 4 was established in the reactions of Me_3SiH with other fragment metal carbonyl negative ions.[19a]

Reductive elimination of H_2 in forming the product ions in eq 3a and 4 is consistent with the structure of the ions at *m/z* 154 being the 15-electron product of cyclopropane C–H bond oxidative insertion, $(OC)_2Fe(H)(\eta^1\text{-}c\text{-}C_3H_5)^{\bullet-}$ (**1**).[17,19a] This structural assignment was confirmed in the reaction of the *m/z* 154 ions with D_2 where *a single H/D exchange was observed* (eq 5). The

$$\underset{m/z\ 154}{(OC)_2Fe(H)(c\text{-}C_3H_5)^{\bullet-}} + D_2 \rightarrow$$

$$\underset{m/z\ 155}{(OC)_2Fe(D)(c\text{-}C_3H_5)^{\bullet-}} + HD \quad (5)$$

results of reactions 3–5 establish the presence of a Fe–H bond in the coordinatively unsaturated adduct product formed in reaction 1a.

The reactions of the (adduct–H_2) product ions at *m/z* 152 (eq 1b) with H_2S[17] and Me_3SiH[19a] produced exclusively the corresponding adduct ions at *m/z* 186 and 226, respectively. No reaction was observed between the *m/z* 152 ions and D_2. These results require that the (adduct–H_2) product ions of eq 1b are 15-electron species without Fe–H or exchangeable C–H bonds. The structures considered most reasonable for these ions are the π-cyclopropene complex **2**, formed via a β-hydride shift from **1** followed by ejection of H_2, and the cyclopropylidene complex **3**, involving an α-hydride migration from **1** and loss of H_2.

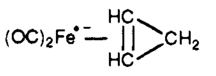

2

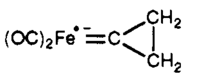

3

The above results of the ion/molecule reactions of the (adduct–H_2) ions at *m/z* 152 do not clearly distinguish between structures **2** and **3**. However, we favor structure **2** for these unsaturated ions by analogy with the β-dehydrogenation of alkanes and cycloalkanes by $(OC)_2Fe^{\bullet-}$ and $(OC)_3Mn^-$,[17] and the high preference for β- rather than α-hydride shifts in related anionic intermediates.[21] That H/D exchange is not observed in the reaction of the *m/z* 152 ions with D_2 suggests that D_2 does not add to the Fe center of **2** within the several millisecond time frame of the experiment. The rate constants for addition of H_2 and D_2 to several 15-electron Fe-centered complex negative ions are frequently smaller by a factor of ≥100 than the rate constants for the related reactions with H_2S and Me_3SiH.[22] If D_2 could add to the metal center of **2**, we would expect to see up to four H/D exchanges in the organic ligand, as seen previously for $(OC)_3Mn(\pi\text{-}C_2H_4)^-$.[17]

The structural assignments of the products from reaction 2 also rely on the results of their ion/molecule reactions. Neither ion reacted with D_2, H_2S, or Me_3SiH, suggesting that they are saturated 18-electron species. However, both ions at *m/z* 179 and 181 reacted rapidly with SO_2 ($k_{total} \approx 6.2 \times 10^{-10}$ cm^3 molecule^{-1} s^{-1}) by displacement of the elements of the organic component according to eq 6 and 7. The large rate constant for reaction

$$m/z\ 181 + SO_2 \rightarrow \underset{m/z\ 203}{(OC)_3Mn(SO_2)^-} + H_2 + C_3H_4 \quad (6)$$

$$m/z\ 179 + SO_2 \rightarrow (OC)_3Mn(SO_2)^- + C_3H_4 \quad (7)$$

6 is consistent with ejection of the elements of the original cyclopropane molecule as two units rather than first rearranging and eliminating as cyclopropane. This conclusion is based on our results of the slow reactions of SO_2 with several 18-electron metal complex negative ions related to $(OC)_3Mn(H)(\eta^3\text{-}C_3H_5)^-$.[17] In these latter cases, the small rate constants (50–70 times smaller than those for reactions 6 and 7) were interpreted as requiring rearrangement of the hydrido-(η^3-allyl) ions to $(OC)_3Mn(\pi\text{-}CH_2{=}CHCH_3)^-$ in the collision complex with SO_2 and that a barrier exists for this rearrangement. Structures **4** and **5** for the adduct at *m/z* 181 (eq 2a) are consistent with these results. The present data do not allow us to distinguish between these two structures.

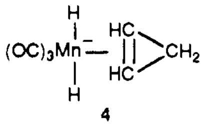

4

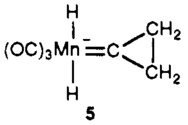

5

Of the several possible 18-electron structures considered for the (adduct–H_2) ions at *m/z* 179 (eq 2b), structure **6** involving a cyclopropenyl ligand is interesting. This unusual ligand could result from **4** by reductive elimination of H_2 followed by insertion of the metal center into an "allylic" C–H bond of the intermediate π-cyclopropene ligand. Since the symmetrical η^3 form of this ligand would suggest that it is derived from the antiaromatic anion $c\text{-}C_3H_3^-$,[23] it may be better viewed as a η^1 ligand to C_1 of the cyclopropenyl group with a distorted π component or vice versa. While we are unable to establish the structure of these (adduct–H_2) product ions from the present data, their formation is more consistent with the structure of the precursor adduct ions at *m/z* 181 being **4** rather than **5**.

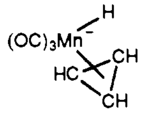

6

Having established the major structural features of the products from reactions 1 and 2, the reaction mechanism can be considered. Since both adduct and (adduct–H_2) ion products are observed, the mechanism consistent with these and the previous results of dehydrogenation of alkanes and cycloalkanes ($c\text{-}C_5H_{10}$ and $c\text{-}C_6H_{12}$)[17] is shown in Scheme I. The loose, orbiting collision complexes at the inlet and outlet channels are omitted for clarity. The mechanism involves initial C–H bond insertion by the metal center forming the excited hydrido-($c\text{-}C_3H_5$) adduct **7*** followed by a β-hydrogen shift yielding the excited dihydrido-($c\text{-}C_3H_4$)

---

[21] McDonald, R. N.; Reed, D. J.; Chowdhury, A. K. *Organometallics* **1989**, *8*, 1122.

[22] McDonald, R. N.; Chowdhury, A. K., unpublished results.

[23] For a brief discussion of this ion, see: March, J.; *Advanced Organic Chemistry*, 3rd ed.; Wiley: New York, 1985; p 53.

Scheme I

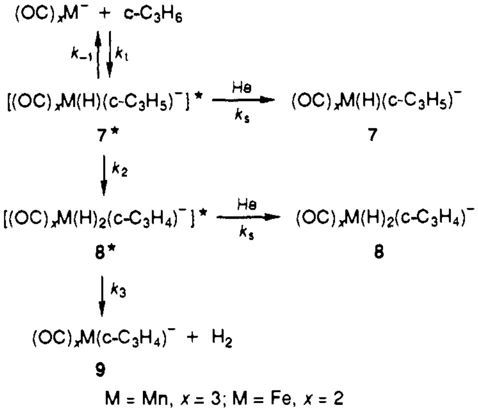

M = Mn, x = 3; M = Fe, x = 2

adduct **8*** and reductive elimination of H_2 to yield the (adduct-H_2) products **9**. The adduct product ions **7** and **8** result from collisional quenching of their excited precursors **7*** and **8***, respectively. Since only a few percent of the collisions generate products, the lifetimes of the excited adducts **7*** may be significantly shorter than 6.3×10^{-8} s, which is the inverse of the collision frequency with helium (k_s[He] = 1.6×10^7 s^{-1} at P_{He} = 0.9 Torr).

The differences in the structures of the adduct and (adduct–H_2) ion products formed in reactions 1 and 2 are interesting; both products from reaction 2 are shown to be coordinatively saturated, while the Fe-derived product ions from reaction 1 are coordinatively unsaturated. This suggests an energy preference for coordination and electronic saturation in the Mn-derived product ions compared to the Fe-derived products, and k_2 (reaction 2) > k_2 (reaction 1).[24] The absence of $(OC)_3Mn(H)(c\text{-}C_3H_5)^-$ as an observable part of the adduct ions in reaction 2 means that k_2 exceeds the collisional quenching of this hydrido-cyclopropyl adduct intermediate.

If we make the reasonable assumption of similar collisional quenching efficiencies for the two adducts $(OC)_xM(H)_2(c\text{-}C_3H_4)^-$,[25] why is it that with M = Fe, x = 2, reductive elimination of H_2 is the ions total fate, while only 20% of the adducts with M = Mn, x = 3, eject H_2 and 80% are collisionally stabilized? We believe that this difference is related to the spin multiplicities of the reactant and product ions in the reductive elimination of H_2 from the corresponding dihydrido-adduct ions. Since the 17-electron $(OC)_2Fe(H)_2(c\text{-}C_3H_4)^{\bullet-}$ intermediate is not observed in reaction 1, this structure must be unstable relative to reductive elimination of H_2. In the reductive elimination $(OC)_2Fe(H)_2(c\text{-}C_3H_4)^{\bullet-} \rightarrow (CO)_2Fe(c\text{-}C_3H_4)^{\bullet-} + H_2$, the 17-electron starting ions and the 15-electron product ions will both have doublet electronic ground states and the reaction is spin allowed.[28] However, ejection of H_2 from the 18-electron singlet ground electronic state of the $(OC)_3Mn(H)_2(c\text{-}C_3H_4)^-$ adduct ions is spin forbidden since the product will be a 16-electron triplet ground-state species.[28] Thus, k_3 (reaction 1) > k_3 (reaction 2).

Table II. Reaction Efficiencies per C–H Bond Type Derived from the Reactions of $(OC)_3Mn^-$ and $(OC)_2Fe^{\bullet-}$ with Certain Acyclic and Cyclic Alkanes

alkane reactant	type of C–H bond	RE/(C–H bond type)	
		$(OC)_3Mn^-$	$(OC)_2Fe^-$
C_2H_6	primary	$1.5 \times 10^{-3\,a}$	$2.5 \times 10^{-3\,a}$
$c\text{-}C_5H_{10}$	secondary	$1.1 \times 10^{-2\,a}$	$2.1 \times 10^{-2\,a}$
$(CH_3)_3CH$	tertiary	$2.0 \times 10^{-2\,a,b}$	$1.5 \times 10^{-2\,a,b}$
$c\text{-}C_3H_6$		$7.0 \times 10^{-3\,c}$	$1.4 \times 10^{-2\,c}$

[a] Reference 17. [b] This value assumed the same RE/(primary C–H bond) for the nine primary C–H bonds in the reactant to be that determined in the reaction with ethane.[17] [c] Present work.

The reactivities of the C–H bonds, defined as (reaction efficiency)/(number of equivalent C–H bonds), of ethane, cyclopentane, 2-methylpropane, and cyclopropane from their reactions with $(OC)_2Fe^{\bullet-}$ and $(OC)_3Mn^-$ are listed in Table II. The RE/($c\text{-}C_3H_5$–H bond) values are about 65% of the RE/(secondary C–H bond) determined from the reactions of the metal carbonyl negative ions with cyclopentane, which previously were found to be representative of secondary C–H bonds in various alkanes.[17] $D°(c\text{-}C_3H_5\text{–}H)$ = 106 kcal mol^{-1} [31] is ≈11 kcal mol^{-1} larger than a typical secondary C–H bond. To overcome this energetic difference requires that the metal–(η^1-cyclopropyl) bond energy is *greater* than the metal–(η^1-(sec-alkyl)) bond energy by as much as 11 kcal mol^{-1} in these negative ion complexes. This increased bond strength of the cyclopropyl ligand is likely due to a larger contribution in the σ bond as well as in the π-back-bonding from the metal to a pseudo-π^* MO of cyclopropane.

Reactions with Cyclopropane-d_6. The observation of the adduct as well as the (adduct–H_2) product ions in reactions 1 and 2 prompted the determination of kinetic deuterium isotope effects for these two reactions. The deuterium isotope effects measured for the dehydrogenation of ethane and $c\text{-}C_6H_{12}$ with $(OC)_3Mn^-$ ($k_{C_2H_6}/k_{C_2D_6}$ = 2.2 ± 0.2, $k_{c\text{-}C_6H_{12}}/k_{c\text{-}C_6D_{12}}$ = 3.4 ± 0.8) and $(OC)_2Fe^{\bullet-}$ ($k_{C_2H_6}/k_{C_2D_6}$ = 3.2 ± 0.2, $k_{c\text{-}C_6H_{12}}/k_{c\text{-}C_6D_{12}}$ = 5.0 ± 0.8) were the weighted averages of the isotope effects for the separate steps of oxidative insertion into the C–H bond of the hydrocarbon and the intramolecular β-hydrogen shift since *both steps* were shown to control the rate constants.[17,32] Thus, the results from reactions 1 and 2 offered the possibility to examine each of these steps separately.

The product results from the reactions of $(OC)_2Fe^{\bullet-}$ and $(OC)_3Mn^-$ with cyclopropane-d_6 are shown in eq 8 and 9 with

$$\underset{m/z\ 112}{(OC)_2Fe^{\bullet-}} + c\text{-}C_3D_6 \xrightarrow[\approx 0.80]{He} \underset{m/z\ 160}{(OC)_2Fe(D)(c\text{-}C_3D_5)^{\bullet-}} \quad (8a)$$

$$\xrightarrow[\approx 0.09]{He} \underset{m/z\ 160}{(OC)_2Fe(D)_2(c\text{-}C_3D_4)^{\bullet-}} \quad (8b)$$

$$\xrightarrow[0.11]{} \underset{m/z\ 156}{(OC)_2Fe(C_3D_4)^{\bullet-}} + D_2 \quad (8c)$$

$$\underset{m/z\ 139}{(OC)_3Mn^-} + c\text{-}C_3D_6 \xrightarrow[\approx 0.80]{He} \underset{m/z\ 187}{(OC)_3Mn(D)_2(c\text{-}C_3D_4)^-} \quad (9a)$$

$$\xrightarrow[\approx 0.20]{He} \underset{m/z\ 187}{(OC)_3Mn(D)(c\text{-}C_3D_5)^-} \quad (9b)$$

the rate constants listed in Table I. Comparing the branching fractions of reactions 2 and 9, we see that the minor amount (20%) of reductive elimination of H_2 yielding the (adduct–H_2) in eq 2b

---

(24) This point was not apparent in the previous studies of the dehydrogenation of n-alkanes, $c\text{-}C_5H_{10}$, and $c\text{-}C_6H_{12}$ with these two fragment metal carbonyl negative ions.[17] In those studies, the Mn-derived products from reactions with alkanes and cycloalkanes containing allylic C–H bonds adjacent to the β-dehydrogenation site were characterized as 18-electron $(OC)_3Mn(H)(\eta^3\text{-allylic})^-$ complexes. However, we were not able to characterize the Fe-derived (adduct–H_2) product ions as 15- or 17-electron species.[17]

(25) The same collisional quenching efficiencies (70 ± 5%) have been measured for $(OC)_4(O^{13}C)Mn^-$ and $(OC)_3(O^{13}C)Fe^{\bullet-}$ formed in the addition/substitution reactions of ^{13}CO with $(OC)_4Mn^{-\,26}$ and $(OC)_3Fe^{\bullet-}$,[27] respectively.

(26) McDonald, R. N.; Schmidt, M. A. Unpublished results.

(27) McDonald, R. N.; Bianchina, E. J. *Organometallics* **1991**, *10*, 1274.

(28) The electronic ground states of the metal carbonyl negative ions complexes $(OC)_{4,3}Mn^-$ (triplets) and $(OC)_{3,2}Fe^{\bullet-}$ (doublets) were assigned based on their rate constants for the reactions with alkenes, dienes, acetylene, benzene, trimethylsilane, silane, and germane.[19] The rate constants for $(OC)_4Mn^-$ forming 18-electron, singlet adducts with these reagents were significantly smaller than those for the reactions of the other three anion complexes. $(OC)_4Mn^-$ is isoelectronic with $Fe(CO)_4$ that is known experimentally[29] and theoretically[30] to have a triplet electronic ground state.

(29) Barton, T. J.; Grinter, R.; Thomson, A. J.; Davies, B.; Poliakoff, M. *J. Chem. Soc., Chem. Commun.* **1977**, 841.

(30) Burdett, J. *J. Chem. Soc., Faraday Trans. 2* **1974**, *70*, 1599.

(31) Baghal-Vayjooee, M. H.; Benson, S. W. *J. Am. Chem. Soc.* **1979**, *101*, 2838.

(32) Melander and Saunders (Melander, L.; Saunders, W. H. *Reaction Rates of Isotopic Molecules*; Wiley-Interscience: New York, 1980) point out that the isotope effect for reactions involving sequential steps where more than one step controls the rate is a *weighted average* of the isotope effects of those steps.

is absent in the reaction with cyclopropane-d_6. Even more remarkable is the conversion of 83% of the product ions from the major elimination channel 1b into the deuterated adduct product ions at m/z 160 in reaction 8.

Approximately 90% of the adduct ions from reaction 8 are assigned the unsaturated deuterio-(c-C_3D_5) structure since these ions added Me_3SiH and ejected HD. The remaining unreactive adduct ions at m/z 160 are considered to have the dideuterio-(c-C_3D_4) structure (eq 8b). The (adduct–D_2) ions at m/z 156 (eq 8c) added Me_3SiH to form their corresponding adducts. Approximately 20% of the adduct product ions at m/z 187 from reaction 9 were observed to react with Me_3SiH by addition followed by loss of HD, suggesting that these ions were the deuterio-cyclopropyl adduct ions. The remaining adduct ions that did not react with Me_3SiH are assumed to be the 18-electron dideuterio complexes shown in eq 9a.

Deuterium Isotope Effects. The rate constant ratio $k_{c\text{-}C_3H_6}/k_{c\text{-}C_3D_6}$ for the reactions with $(OC)_2Fe^{\bullet-}$ is 1.2 ± 0.1. The small magnitude of this kinetic isotope effect differs considerably from that reported for the rate-limiting oxidative insertion by Co^+ into the C–H bonds of propane where $k_{C_3H_8}/k_{C_3D_8} = 2.8 \pm 0.8$ under single collision conditions.[33] The efficiency of the Co^+/C_3H_8 reaction is 0.13. The kinetic bottleneck is a significant barrier for the C–H bond oxidative insertion step located 0.11 eV below the entrance channel asymptotic energy. Once formed, the two egoergic product forming channels of dehydrogenation and demthanation are available to remove the excited $[Co(H)(C_3H_7)^+]^*$ ions; the ratio for the loss of H_2 and CH_4 is ≈3 at a kinetic energy of 0.05 eV C.M. The reaction of Co^+ with C_3D_8 decreases the cross sections for both H_2 and CH_4 loss channels by the same amount. The efficiency of the Co^+/C_3H_8 reaction is increased to 0.83 under the multicollision, higher pressure conditions ($P_{He} = 0.75$ Torr, 300 K) of a flow reactor yielding 95% of the adduct along with small amounts of ion products formed by loss of H_2 and CH_4 (3/1).[34]

We suggest that the small kinetic deuterium isotope effect observed in the reactions of $(OC)_2Fe^{\bullet-}$ with c-C_3H_6 and c-C_3D_6 is the result of the larger number of low-energy vibrations present in the excited intermediate deuterated adduct ions. This leads to an increased density of states and lifetime[35] of the **7***-d_6 (M = Fe, x = 2) ions. If the collisional quenching only involved the stabilization of the excited deuterio-(c-C_3D_5) and dideuterio-(c-C_3D_4) intermediate ions that as protio complexes formed adduct and (adduct-H_2) ions, respectively, we would have expected to see a significantly larger isotope effect than was observed. This would be due to the normal isotope effects for the bimolecular oxidative insertion step, k_1, and the intramolecular deuterium shift, k_2, for those ions that proceed via this step.[32]

The **7***-d_6 (M = Fe, x = 2) ions are partitioned by three channels: (a) c-C_3D_6 reductive elimination, k_{-1}; (b) a deuterium shift followed by elimination of D_2, k_2 and k_3; and (c) collisional quenching, k_s[He]. The product branching fractions of reactions 8a and 1a (ratio ≈2.3) demonstrate the large increase in the collisional quenching efficiency of the deuterated intermediates **7***-d_6 (M = Fe, x = 2) compared to the protio complexes **7***. The greater efficiency of collisional quenching removes a larger fraction of **7***-d_6 ions from the smaller flux of excited deuterated adducts produced because of the normal isotope effect on k_1 in reaction 9. This can be facilitated by an expected normal isotope effect on k_{-1}; the reductive elimination of alkanes from $L_nM(H)(R)$ complexes in the condensed phase exhibit normal deuterium isotope effects in the range of 2.2–3.3.[13b] By significantly increasing the efficiency of the quenching process (c), the rates of the competing unimolecular processes (a) and (b) will be decreased. The important result in the present context is a reduction in the fraction of **7***-d_6 (M = Fe, x = 2) ions that return via the inlet channel, k_{-1}, in reaction 8.[36] This increases k_{total} for reaction 8 and the rate ratio $k_{c\text{-}C_3H_6}/k_{c\text{-}C_3D_6}$ approaches unity.

The ratio of the rate constants for the corresponding reactions of $(OC)_3Mn^-$ with c-C_3H_6 and c-C_3D_6 is 1.9 ± 0.3. The major process in reaction 9 is that of collisional quenching of the saturated dideuterio-(c-C_3D_4) adducts (similar to the major product channel in reaction 2) along with ≈20% of the unsaturated deuterio-(c-C_3D_5) adduct ions. Assuming similar collisional quenching efficiencies for the excited adducts $[(OC)_3Mn(D)(c\text{-}C_3D_5)^-]^*$ and $[(OC)_2Fe(D)(c\text{-}C_3D_5)^{\bullet-}]^*$[25], a small isotope effect, similar to that found for the $(OC)_2Fe^{\bullet-}$ reactions, would be expected *if* reaction 9 terminated at the deuterio-(c-C_3H_5) adduct structure. However, the major adduct ions result from the additional step of intramolecular deuterium migration from carbon to the metal center. Since deuterium prefers bonding to carbon rather than to a metal from zero-point energy considerations,[37] a normal isotope effect is expected for k_2 which reduces the flux of **8***-d_6 (M = Mn, x = 3) ions. We believe that it is the isotope effect of this additional step which increases the observed isotope effect for the $(OC)_3Mn^-$ reactions compared to that found with $(OC)_2Fe^{\bullet-}$.

The above analyses of the results do not allow for the extraction of the individual kinetic deuterium isotope effects for the steps in Scheme I for the two metal carbonyl negative ions. However, the present results (i) confirm the involvement of the intermediates **7*** and **8*** in the mechanism for the dehydrogenation of alkanes and cycloalkanes by $(OC)_3Mn^-$ and $(OC)_2Fe^{\bullet-}$, (ii) confirm the contribution of the rate constants for oxidative insertion and the intramolecular hydrogen shift steps to k_{total} for the reaction, and (iii) establish the presence of the return of $[(OC)_xM(H)(R)^-]^*$ adduct ions to the starting ion and neutral RH, k_{-1}.

The rate and product data in Table I clearly illustrate a problem for the measurement of kinetic deuterium isotope effects in the gas phase under multicollision conditions where adduct formation is a significant product-forming channel. The multicollision conditions will produce "inflated" rate constants for the deuterated substrate that mask the true magnitude of the kinetic isotope effect. To avoid this problem, these data should be obtained under single collision conditions. However, care must be taken at the low pressures required for single collision conditions to remove excited electronic states of the starting ions.

Summary

The reactions of $(OC)_2Fe^{\bullet-}$ and $(OC)_3Mn^-$ with cyclopropane have been shown to occur exclusively by initial oxidative insertion of the metal center into a cyclopropyl-H bond. The products were different amounts of adduct and (adduct–H_2) ions. The structures of the product ions were assigned based on the results of their reactions with various neutral substrates, e.g., D_2, Me_3SiH, and H_2S. Both the adduct and (adduct–H_2) product ions (amount formed) from the $(OC)_2Fe^{\bullet-}$ reaction reacted readily with these neutrals and are assigned the unsaturated structures $(OC)_2Fe(H)(c\text{-}C_3H_5)^{\bullet-}$ (35%) and $(OC)_2Fe(c\text{-}C_3H_4)^{\bullet-}$ (65%), respectively. The suggested structures of the adduct and (adduct–H_2) products from the $(OC)_3Mn^-$ reaction are the saturated complexes $(OC)_3Mn(H)_2(c\text{-}C_3H_4)^-$ (80%) and $(OC)_3Mn(H)(\eta^3\text{-}c\text{-}C_3H_3)^-$ (20%), respectively, due to their failure to react with these reagents.

The corresponding reactions of the two fragment metal carbonyl negative ions with c-C_3D_6 generated significantly larger amounts of the adduct product ions and reduced amounts of the (adduct–D_2) ions. The products from the $(OC)_2Fe^{\bullet-}$ reaction were identified as two adducts, $(OC)_2Fe(D)(c\text{-}C_3D_5)^{\bullet-}$ (≈80%) and $(OC)_2Fe(D)_2(c\text{-}C_3D_4)^{\bullet-}$ (≈9%), and the (adduct–D_2), $(OC)_2Fe$-

---

[33] van Koppen, P. A. M.; Brodbelt-Lustig, J.; Bowers, M. T.; Dearden, D. V.; Beauchamp, J. L.; Fisher, E. R.; Armentrout, P. B. *J. Am. Chem. Soc.* **1991**, *113*, 2359.

[34] Tonkyn, R. T.; Ronan, M.; Weisshaar, J. C. *J. Phys. Chem.* **1988**, *92*, 92.

[35] The lower limits of the lifetimes of the adducts formed in the reaction of Co^+ with C_3H_8 and C_3D_8 differ by a factor of almost 4.[29]

[36] The efficiency of reaction 2 is low at 0.08. Assuming a simplified model for reaction 9 involving rate-limiting C–H bond oxidative insertion with an isotope effect of 2, the quenching efficiency of the intermediate **1***-d_6 ions must be twice that for quenching the protio **1*** ions to give no net isotope effect.

[37] For the IR stretching frequencies of metal-hydrogen bonds, ν_{MH} 2300–1600 cm^{-1} (Collman, J. P.; Hegedus, L. S.; Norton, J. R.; Finke, R. G. *Principles and Applications of Organotransition Metal Chemistry*; University Science Books: Mill Valley, CA, 1987; p 83) and ν_{MH} 2300–1700 cm^{-1} (Kubas, G. J. *Acc. Chem. Res.* **1988**, *21*, 120).

$(c\text{-}C_3D_4)^{\bullet -}$ (11%). Only the two adducts $(OC)_3Mn(D)(c\text{-}C_3D_5)^-$ ($\approx$20%) and $(OC)_3Mn(D)_2(c\text{-}C_3D_4)^-$ ($\approx$80%) were formed in the reaction with $(OC)_3Mn^-$.

The small kinetic isotope effects observed for the $(OC)_2Fe^{\bullet -}$ (1.2 ± 0.1) and $(OC)_3Mn^-$ reactions (1.9 ± 0.3) suggest the intervention of secondary isotope effects that *increase* the rate constants of the cyclopropane-d_6 reactions. The secondary effects are the increase in the density of states and lifetimes of the excited deuterated adducts that result in an increase in the collisional quenching efficiency of these species. The larger quenching efficiency not only influences the yields of the intermediates involved in the product channel, but reduces the extent of the reductive elimination of cyclopropane-d_6 from $\mathbf{7}^*\text{-}d_6$ (k_{-1}). It is this latter factor that inflates k_{total} for the cyclopropane-d_6 reactions and masks the isotope effect for the oxidative insertion step. This is most clearly seen in the results of the $(OC)_2Fe^{\bullet -}$ reaction with cyclopropane-d_6, where the major product ions are those formed in the initial intermolecular step. The larger isotope effect observed for the $(OC)_3Mn^-$ reactions arises because the major product adduct ions result from the additional step of an intramolecular deuterium shift (k_2) and its attendant normal isotope effect.

The present results are consistent with the available data on the reactions of $(OC)_2Fe^{\bullet -}$ and $(OC)_3Mn^-$ with alkanes and other cycloalkanes,[17] and establish the intermediacy of the related $\mathbf{7}^*$ and $\mathbf{8}^*$ ions in the mechanism of dehydrogenation of these substrates.

Acknowledgment. The authors are pleased to acknowledge the financial support of the National Science Foundation for this research.

Registry No. 1, 137007-86-4; **1**-d_6, 137007-88-6; **2**, 137007-87-5; **2**-d_4, 137007-89-7; **4**, 137007-90-0; **4**-d_6, 137007-92-2; **6**, 137007-91-1; $(CO)_3Mn^-$, 101953-17-7; $(CO)_2Fe^{\bullet -}$, 71701-39-8; $c\text{-}C_3H_6$, 75-19-4; $c\text{-}C_3D_6$, 2207-64-9.

Application of the Xenon-Adsorption Method for the Study of Metal Cluster Formation and Growth on Y Zeolite

Ryong Ryoo,[*] Sung June Cho, Chanho Pak, Jeong-Guk Kim,[†] Son-Ki Ihm,[†] and Jeong Yong Lee[‡]

Department of Chemistry and Center for Molecular Science, Department of Chemical Engineering, and Department of Materials Science and Engineering, Korea Advanced Institute of Science and Technology, Taeduk Science Town, Taejon, 305-701 Korea.

Received March 12, 1991

Abstract: Supported metal clusters of Pt, Ir, Ru, Rh, and Pd have been prepared in the supercage of Y zeolite by activating their ion-exchanged ammine complexes. Xenon adsorption isotherms obtained from these samples at temperatures ranging from 296 to 340 K and pressures up to 500 Torr, as well as the chemical shift data from the ^{129}Xe NMR study of the adsorbed xenon gas, indicate that the xenon adsorption can occur quite strongly, becoming saturated above ca. 50 Torr, on the metal cluster surface whereas the adsorption is so weak on the support that the adsorbed quantity increases linearly with pressure according to Henry's law. Upon chemisorption of hydrogen or oxygen, the metal clusters lose the ability to adsorb the xenon so strongly, resulting in a decrease in the xenon adsorption quantity. Such a xenon-adsorption decrease due to the chemisorption of another gas can determine the amount of xenon that can be saturated on all the metal clusters present in the sample. This quantity is sensitive to the size and the number of the supported clusters. It can then be used to probe the formation and the size variation of the clusters which are very difficult to study by other methods due to their very small size, e.g. about 1 nm. An application of such a simple technique for the study of Pt cluster formation on NaY zeolite indicates that the size of the Pt cluster formed in the supercage does not change significantly as the metal content is changed from 2 to 10%. This xenon-adsorption method has also been very useful for the study of the formation and growth of the Ru cluster on NaY zeolite. The result indicates that very small Ru clusters are formed in the supercage by treating a precursor, which is prepared by heating NaY zeolite in an aqueous ammonia solution of $RuCl_3$, in vacuum at temperatures above 623 K. The clusters grow gradually at higher temperatures both in H_2 and under vacuum. The data also agree that an exposure of the supported Ru clusters in O_2 at temperatures above 423 K causes excessive migration of the Ru species, resulting in large agglomeration. Another example, which can further promise wide applicability of the xenon adsorption method, is a study of the formation of Pd clusters in the supercage of various ion-exchanged Y and X zeolites. The result indicates that Ca^{2+}, Y^{3+}, and perhaps other multivalent cations residing in the supercage are necessary to obtain ca. 1-nm clusters whereas univalent cations give larger clusters.

Introduction

Metal clusters supported on Y zeolite, of ca. 1 nm, can be a suitable subject for the adsorption and catalysis of very small clusters.[1] The effect of the cluster-size variation on the chemisorptive and catalytic properties of the small metal cluster is particularly interesting since its understanding may build a bridge between homogeneous catalysis and heterogeneous catalysis. However, such a study requires a very precise method to determine the cluster size to the level of the number of atoms per cluster. A few approaches for the determination of the average number of metal atoms per cluster supported on Y zeolites using certain assumptions have been reported,[2,3] but in general their results failed to agree with those obtained by other methods such as transmission electron microscopy (TEM),[4-6] extended X-ray absorption fine

---

[*] Author to whom correspondence should be addressed at the Department of Chemistry.

[†] Department of Chemical Engineering.

[‡] Department of Materials Science and Engineering.

(1) Jacobs, P. A. In *Metal Clusters in Catalysis*; Gates, B. C., Guczi, L., Knozinger, H., Eds.; Elsevier: Amsterdam, 1986; p 357.

(2) Dalla Betta, R. A.; Boudart, M. In *Proceedings of the 5th International Congress on Catalysis, Palm Beach*; Hightower, J., Ed.; North Holland: Amsterdam, 1973; Vol. 2, p 1329.

(3) de Menorval, L.-C.; Fraissard, J. P.; Ito, T. *J. Chem. Soc., Faraday Trans. 1* **1982**, *78*, 403.

(4) Gallezot, P.; Mutin, I.; Dalmai-Imelik, G.; Imelik, B. *J. Microsc. Spectrosc. Electron* **1976**, *1*, 1.